Self-Assembled Fmoc-Peptides as a Platform for the Formation of Nanostructures and Hydrogels

Ron Orbach,[†] Lihi Adler-Abramovich,[†] Sivan Zigerson,[‡] Iris Mironi-Harpaz,[‡] Dror Seliktar,[‡] and Ehud Gazit*,[†]

Department of Molecular Microbiology and Biotechnology, George S. Wise Faculty of Life Sciences, Tel-Aviv University, Tel-Aviv 6407536, Israel, and Faculty of Biomedical Engineering, Technion - Israel Institute of Technology, Haifa 32000, Israel

Received May 22, 2009; Revised Manuscript Received August 5, 2009

Hydrogels are of great interest as a class of materials for tissue engineering, axonal regeneration, and controlled drug delivery, as they offer 3D interwoven scaffolds to support the growth of cells. Herein, we extend the family of the aromatic Fmoc-dipeptides with a library of new Fmoc-peptides, which include natural and synthetic amino acids with an aromatic nature. We describe the self-assembly of these Fmoc-peptides into various structures and characterize their distinctive molecular and physical properties. Moreover, we describe the fabrication of the bioactive RGD sequence into a hydrogel. This unique material offers new opportunities for developing cell-adhesive biomedical hydrogel scaffolds, as well as for establishing strategies to modify surfaces with bioactive materials.

Introduction

The molecular self-assembly process of biological building blocks enables the formation of complex architectures and machinery; hence, it offers a new direction for the design and fabrication of novel materials that can be used in various applications, such as, microelectronics, microelectromechanical systems (MEMS), drug delivery, and tissue engineering.[1−6] Designed and well-ordered structures can be formed by in vitro self-assembly of nucleic acids, phospholipids, and polypeptide building blocks.[7−10] Diverse chemical and structural species integrated into proteins and polypeptides may confer upon them some advantages over other building blocks for constructing complex architectures.[2,4,11−13] One example is the use of simple proteins as templates for the fabrication of metallic nanowires by using molecular-biology tools to insert metal-binding elements into the protein sequences.[14] Similar to proteins and large polypeptides, short peptides can also self-assemble into various nanostructures such as spheres, tubes, and tapes.[7,15−23] These nanostructures can form unique materials at macroscopic as well as nanoscopic scales, such as, nanoscale ordered hydrogels.[24−28]

Hydrogels are frequently used as 3D scaffolds to support the growth of cultured cells for tissue engineering and regeneration.[29−31] A variety of natural polymers may be used as hydrogel-forming materials. These polymers are appealing for medical use owing to their similarity to the natural extracellular matrix (ECM), which allows cell adhesion while maintaining very good biocompatible and biodegradable properties.[32] Protein- or peptide-based scaffolds represent a very important biocompatible group of materials that can support cell growth.[24−26,28,33,34] Peptide-based hydrogels exhibit the advantages of both synthetic and naturally derived hydrogel forming materials. They are easy to manufacture in large quantities and can also be easily decorated chemically and biologically. Such decoration gives the ability to design an ultrastructure that presents ligands, as well as other biological functional groups, hence, promoting cell adhesion and growth.[33,34] The study of the gelation process of short peptides with an aromatic nature is highly essential. It had been found that the cell nuclear pore complexes are equipped with permeability barriers, which contain short clusters of aromatic amino acids, such as, Phe-Ser-Phe-Gly (FSFG). Those clusters form 3D meshwork with hydrogel-like properties, which enable the nuclear pores' specificity.[35] In their pioneering work, Zhang and colleagues described the use of short peptides with alternating charged and hydrophobic amino acids to generate hydrogels for cultures of various cell lines.[34] Their later work showed the ability of these peptides to form axonal growth through a site of treated lesion and the return of functional vision.[36] Stupp and co-workers showed selective differentiation of neural progenitor cells by the bioactive peptide Ile-Lys-Val-Ala-Val (IKVAV) modified with spacers and aliphatic tails which spontaneously form nanofibrous scaffolds.[33] In 1995, Vegners et al. reported for the first time the formation of hydrogels with fluorenylmethoxycarbonyl (Fmoc)-protected amino acids and dipeptides.[37] The Fmoc moiety is widely used as a protecting group in peptide synthesis and it was even reported by Burch et al. that a number of Fmoc-amino acids show anti-inflammatory properties.[38]

We previously reported the efficient self-assembly, under mild conditions, of the Fmoc-Phe-Phe (Fmoc-FF) into a rigid hydrogel with remarkable physical properties.[39] We suggested that aromatic interactions may have a key role in the formation of tubular structures, as they contribute free energy of formation, as well as order and directionality to the self-assembly process. This suggestion was supported by a parallel independent work done by Ulijn et al., which used spectroscopic techniques to show that Fmoc-FF forms fiber structures due to the formation of antiparallel β-sheets. The β-sheets are stabilized by the fluorenyl groups that are on alternating sides.[40] In this study we extend the family of the aromatic Fmoc-dipeptides[39,40,42,43] with a library of new Fmoc-peptides. We characterize their distinctive molecular and physical properties as well as examine their possible use in vitro, using a cell culture model.

* To whom correspondence should be addressed. E-mail: ehudg@post.tau.ac.il.
[†] Tel-Aviv University.
[‡] Technion - Israel Institute of Technology.

10.1021/bm900584m CCC: $40.75
Published on Web 08/25/2009

Materials and Methods

Hydrogels and Solution Preparation. Lyophilized Fmoc-FF, Fmoc-β-(2-naphthyl)-L-alanine (Fmoc-2-Nal), Fmoc-phenylalanine-proline (Fmoc-FP), Fmoc-phenylalanine-serine(tBu) (Fmoc-FS(tBu)), Fmoc-phenylalanine-glycine (Fmoc-FG), Fmoc-glycine-phenylalanine (Fmoc-GF) (Bachem, Bubendorf, Switzerland), Fmoc-arginine-glycine-aspartic acid (Fmoc-RGD), Fmoc-phenylalanine-arginine-glycine-aspartic acid (Fmoc-FRGD), and Fmoc-arginine-glycine-aspartic acid-phenylalanine (Fmoc-RGDF) (Peptron, Daejeon, South Korea) were dissolved in dimethyl sulfoxide (DMSO) at concentrations of 100 or 25 mg mL^{-1}. The hydrogels were prepared by diluting the stock solution in ultra pure water (Biological Industries, Beit Haemeck, Israel) at a final peptide concentration of 5 mg mL^{-1}. Different hydrogel concentrations were prepared by using different peptide-solution-to-water ratios. To avoid any preaggregation and premature assembly, the stock solutions were prepared fresh for each experiment.

Congo Red Staining and Birefringence. A 20 μL aliquot was allowed to dry on a glass microscope slide. Staining was performed by the addition of a solution of 80% ethanol saturated with congo red and NaCl. Birefrigence was determined with a SZX-12 Stereoscope (Olympus, Hamburg, Germany) equipped with a polarizing stage.

Rheological Analysis. The in situ hydrogel formation, mechanical properties, and cross-linking kinetics were characterized by an AR-G2 rheometer (TA Instruments). Time-sweep oscillatory tests in parallel-plate geometry were performed on 210 μL of fresh solution (resulting in a gap size of 0.6 mm), 1 min after its preparation, at room temperature. Each Fmoc-peptide was tested six times and their average is shown. Oscillatory strain (0.01−100%) and frequency sweeps (0.01−100 Hz) were conducted to find the linear viscoelastic region, wherein the time sweep oscillatory tests were performed.

Fourier Transform Infrared (FTIR) Spectroscopy. FTIR spectra were collected using a Nicolet Nexus 470 FTIR spectrometer with a DTGS (deuterated triglycine sulfate) detector. Hydrogel samples were formed directly on a CaF_2 plate, resuspended with D_2O, and vacuum-dried. Measurements were taken using a 4 cm^{-1} resolution and by averaging 2000 scans. The absorbance maxima values were determined using an OMNIC analysis program (Nicolet). The obtained absorption spectra were smoothed by applying the Savitzky-Golay function to eliminate noise and operating the second derivative transformation on the spectra using the Peakfit software version 4.12 (SYSTAT Software Inc., Richmond, CA).

Transmission Electron Microscopy (TEM) Analysis. A total of 100 μL of hydrogel was prepared and a part of it was placed on a 400-mesh copper grid. After 1 min, the piece of gel and excess fluid were removed. Negative staining was obtained by covering the grid with 10 μL of 2% uranyl acetate in water. After 2 min, excess uranyl acetate solution was removed. Samples were viewed using a JEOL 1200EX TEM operating at 80 kV.

Scanning Electron Microscopy (SEM) Analysis. A piece of freshly formed gel was placed on a microscope glass coverslip, dried at room temperature, and then spattered with gold. Images were obtained with a JSM JEOL 6300 SEM operating at 5.0 kV.

Atomic Force Microscopy (AFM) Analysis. For AFM analysis, an aliquot of low concentration hydrogel was deposited on freshly cleaved mica surface. The samples were probed by a Digital Instrument (DI) MultiModeTM NanoScope IV AFM, using Mikromasch NSC15/Si3N4 cantilever (resonant frequency $f = 325$ kHz, spring constant $k = 40$ N/m) in a tapping mode.

Viability Analysis. For cell growth in vitro experiments, Chinese hamster ovary (CHO) cells were grown in Dulbecco's Modified Eagle Medium (DMEM) supplemented with 10% fetal calf serum, 100 U mL^{-1} penicillin, 100 U mL^{-1} streptomycin, and 2 mmol L^{-1} L-glutamine (all from Beit Haemeck, Israel). Cells were maintained at 37 °C in a humidified atmosphere containing 5% CO_2. Subconfluent cells were harvested by trypsinization, counted, and diluted in the culture medium to 2×10^5 cells mL^{-1}. The hydrogels were swelled overnight with 0.1 mL DMEM. The next day, DMEM was removed and 100 μL of the CHO cells (2×10^4 cells) were placed overtop the hydrogel. After a 24 h incubation period at 37 °C, the viability of the cells was determined using a 3-(4,5-dimethylthiazolyl-2)-2,5-diphenyltetrazolium bromide (MTT) assay.[41]

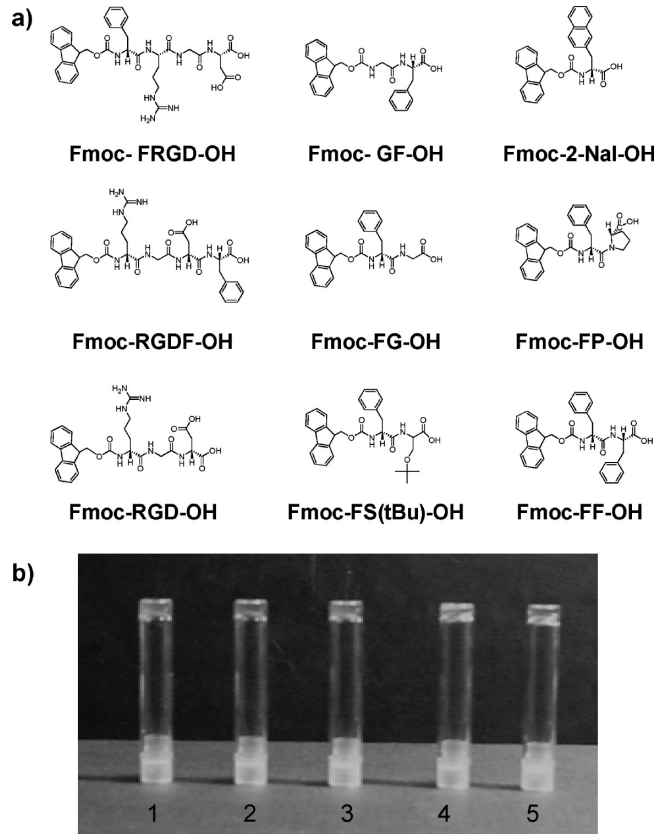

Figure 1. (a) Molecular structure of the nine Fmoc-peptides. (b) A macroscopic image of the hydrogels: (1) Fmoc-FRGD; (2) Fmoc-RGDF; (3) Fmoc-2-Nal; (4) Fmoc-FG; (5) Fmoc-FF.

Results and Discussion

The new library of the Fmoc-peptides includes natural and synthetic amino acids with an aromatic nature (Figure 1). Two of these new Fmoc-peptides designed for enhanced biocompatibility, contained the Arg-Gly-Asp (RGD) sequence. The RGD sequence is a critical part of the cell attachment site in a large number of ECM proteins. As such, it can influence cell migration, growth, differentiation, and apoptosis. The interaction between cell-surface adhesion molecules and ECM proteins can be mimicked using short synthetic peptides containing the RGD sequence. Thus, extensive research has been done on cell−surface interactions with peptide modified biomaterials.[44−47]

Hydrogel Preparation. All the Fmoc-peptides were first dissolved in DMSO and then diluted in water to their final concentration. The dilution of the DMSO solutions into water leads to substantial self-assembly of these peptides. As previously reported by Ulijn and co-workers, Fmoc-FG forms a hydrogel.[43] In addition, Fmoc-FRGD, Fmoc-RGDF, and Fmoc-2-Nal (Figure 1) formed hydrogels, and the gelation process was accompanied by a change in the optical properties of the specimen from a turbid viscous solution (opaque) to a transparent hydrogel. It should be noted that after a few hours, the Fmoc-FG hydrogel contained aggregates and it was not stable for prolonged durations in aqueous solution. Conversely, Fmoc-RGD, Fmoc-Fmoc-FP, Fmoc-FS(tBu), and Fmoc-GF did not form hydrogels and their solution remained turbid, except to

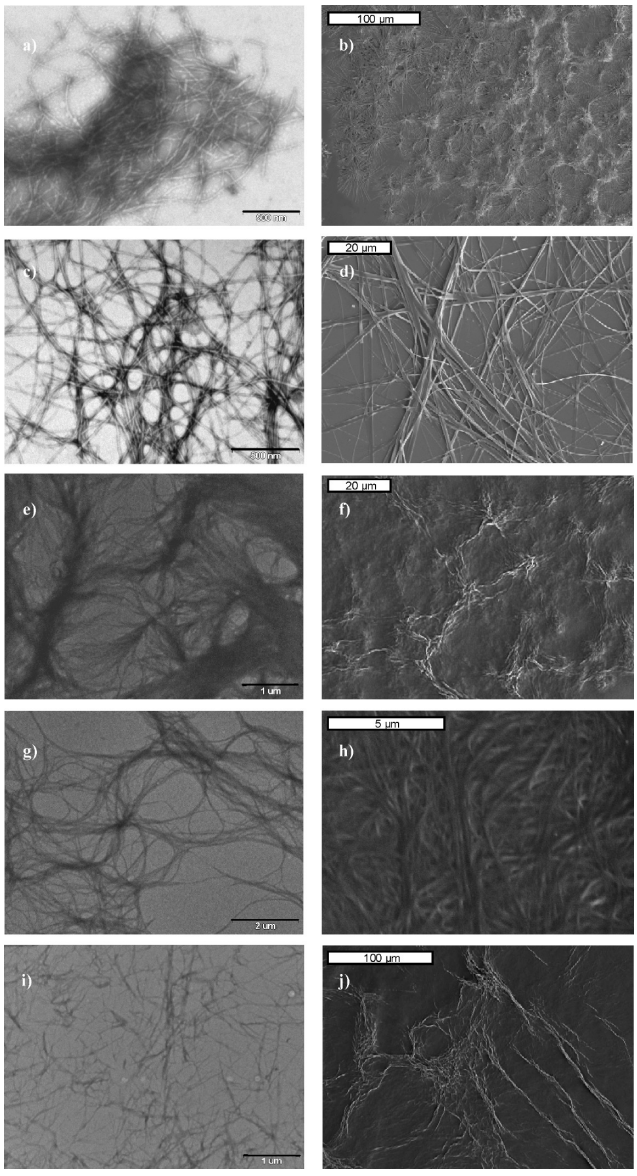

Figure 2. TEM and SEM images of the studied hydrogels: (a,b) Fmoc-2-Nal; (c,d) Fmoc-FG; (e,f) Fmoc-FRGD; (g,h) Fmoc-RGDF; (i,j) Fmoc-FF exhibit tangled fibrous structures.

Fmoc-RGD, which remained clear. However, it should be noted that recently it has been shown that Fmoc-RGD can form a transparent hydrogel at pH = 3.[48] Thus, it appears that the hydrogel formation is pH dependent.

Stability Tests. We tested the stability of the hydrogels in keeping their 3D structure and the ability to support their own weight in an overturned test tube, under extreme pH conditions, by using buffer solutions suspended on the upper side of the hydrogels. Fmoc-FF and Fmoc-2-Nal were stable at broad pH levels (3−12), while Fmoc-FG, Fmoc-FRGD, and Fmoc-RGDF were not stable above pH = 6.5.

Morphology Characterization. To gain more insight about the molecular organization of the self-assembled structures of each peptide, we used TEM and SEM analysis. All Fmoc-peptides that formed hydrogels were arranged as branching, flexible fibrous structures (Figure 2). AFM measurements of the hydrogel structures were conducted for accurate evaluation of their diameter, as the native sample was being tested with no vacuum or external stain, and showed fibers with an average diameter ranging from 10 to 30 nm, for the different Fmoc-peptides (Supporting Information, Figure S1). Fmoc-FP and

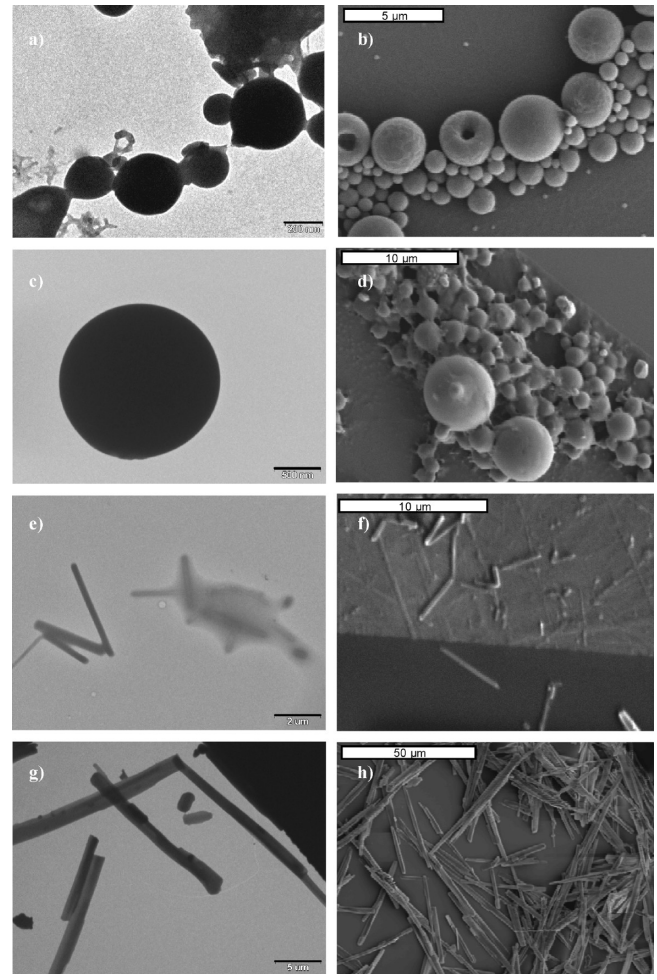

Figure 3. TEM and SEM images of the nonhydrogel forming Fmoc-peptides: (a,b) Fmoc-FP; (c,d) Fmoc-FS(tBu) exhibit spheres; (e,f) Fmoc-RGD; (g,h) Fmoc-GF exhibit discrete tubes.

Fmoc-FS(tBu) formed spheres, whereas Fmoc-RGD and Fmoc-GF formed tubular structures (Figure 3). Based on these results, we suggest that the formation of spheres or tubes does not allow the water to cage and form the hydrogel in the same manner as with the fibrous structure, at the tested conditions. These results also support the notion that the aromatic interactions play a key role in the self-assembly process,[49] which was supported by theoretical studies.[50] Thus, we speculate that the number and location of the aromatic groups in the peptide chain have a direct influence on the structure of the self-assembled product. While Fmoc-FRGD and Fmoc-RGDF, which contain two aromatic moieties (Fmoc and phenylalanine), self-assemble to form a fibrous network, Fmoc-RGD, which contains only one aromatic moiety (Fmoc), forms nanotubes with a very low yield. Additionally, Fmoc-FG, which contains two adjacent aromatic groups also forms a fibrous network, whereas Fmoc-GF forms large tubes having a diameter of several micrometers. Next, we used a birefringence visualization method to further investigate the properties of the observed fibrillar structures. The dehydrated hydrogels and nanostructured peptide assemblies were stained with congo red dye. All of the hydrogels showed some degree of birefringence, indicating on amyloid-like structure, whereas the peptides that did not form hydrogels did not show any birefringence (Supporting Information, Figure S2).

Rheology Characterization. The mechanical properties of the hydrogels are important for determining their suitability in various applications. Hence, rheological characterization was

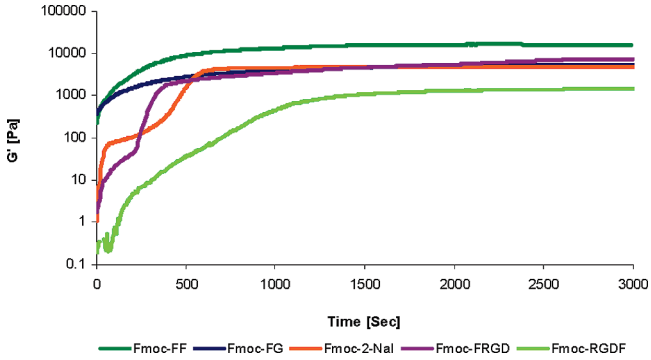

Figure 4. Storage shear modulus of the hydrogel forming Fmoc-peptides.

conducted to study the kinetics of hydrogel formation and the viscoelastic properties of the materials (Figure 4). The complex shear modulus (G^*) of the hydrogels showed that the elastic response component (G', storage modulus) exceeded the viscous response component (G'', loss modulus, not shown) by at least one order of magnitude, indicating a phase transition into a viscoelastic material had taken place. Although the G' values of all the hydrogels reached the plateau value after 30 min, the kinetics of hydrogel formation of each peptide were quite different. The Fmoc-peptides which formed hydrogels the fastest (i.e., G' reached its plateau value the fastest) were Fmoc-FF and Fmoc-FG; with these rapidly forming hydrogels, the rheometry protocol was unable to measure the initial portion of the G' slope associated with the beginning of the phase transition. Fmoc-FRGD, Fmoc-2-Nal, and Fmoc-RGDF all exhibited a slower process of hydrogel phase transition, which was captured almost entirely by the rheometry time-sweep. These results are consistent with the aromatic nature of these peptides; Fmoc-FF and Fmoc-FG have adjacent aromatic moieties and can self-assemble rapidly. Fmoc-RGDF and Fmoc-FRGD have two aromatic moieties on a longer backbone and, hence, may require more time for the molecules to arrange properly during self-assembly to reach their viscoelastic equilibrium. Fmoc-2-Nal exhibits hydrogel formation kinetics similar to the longer peptides, despite its shorter length and two adjacent aromatic moieties; this is possibly owing to steric hindrances caused during self-assembly by the bulky naphthalene systems.

The rheological analysis also showed how the number of aromatic groups and their location on the peptide backbone affected the mechanical properties of the respective hydrogel. Fmoc-FF, which contains three aromatic moieties, showed the highest G'_{plateau} value, indicating that these were the stiffest hydrogels. Fmoc-FG, Fmoc-FRGD, and Fmoc-2-Nal, all having two adjacent aromatic moieties, demonstrated similar G'_{plateau} values, while Fmoc-RGDF exhibited the lowest G'_{plateau} value.

Peptide Mixtures Effect on the Hydrogel Formation Process. Next we formed a mixture of hydrogels using combinations of two different peptides to examine the possibility of precisely controlling the hydrogel's mechanical properties. Interestingly, the Fmoc-FF with Fmoc-2-Nal combination required prolonged times (4 h) for the optical transition to culminate, even though the duration of the optical transition of the individual peptides was after 3.5 and 2 min, respectively. This behavior was also observed for the Fmoc-FF mixed with Fmoc-FG (Supporting Information, Figure S3) that required 1 h for the optical transition to culminate, where the individual peptides showed an optical transition after 3.5 min and 30 s, respectively. In agreement, the rheological data showed that the hydrogel self-assembly kinetics and viscoelastic properties were very different for the mixed solutions when compared to the individual Fmoc-peptides (Supporting Information, Figure S4). It appeared that the hydrogel formation of the individual peptides was a two-step process, whereas the optical transition was mostly evident during the initial step of the hydrogel formation when G' increases exponentially. We hypothesize that the time required for the optical transition corresponds to the duration of the molecules initial organization from many irregular aggregates of dimension at the range of the visible wavelength, into a crystalline form, through the process of self-assembly. Thus, it seems that the slower kinetics of the peptide mixtures may be the result of the intricacies of forming more complex supermolecular structures made from the two types of peptides or, alternatively, it may be due to the diffusional effects involved in the coformation of two distinct populations.

Table 1. Morphological Properties of the Various Fmoc-Peptides

compound	structure	diameter	hydrogel	secondary structure
Fmoc-FF-OH	fibrous	10−30 nm	√	β-sheet
Fmoc-FG-OH	fibrous	10−30 nm	√	non-β-sheet
Fmoc-2-Nal	fibrous	10−30 nm	√	β-sheet
Fmoc-GF-OH	microtubes	1− 5 μm	×	
Fmoc-FRGD-OH	fibrous	10−30 nm	√	β-sheet
Fmoc-RGDF-OH	fibrous	10−30 nm	√	β-sheet
Fmoc-RGD-OH	nanotubes	10−20 nm	×	
Fmoc-FS(tBu)-OH	spheres	20 nm−20 μm	×	
Fmoc-FP-OH	spheres	20 nm−20 μm	×	

Secondary Structure Studies. Next we examined the nature of the secondary structures of the nanoassemblies using FTIR spectroscopy. Fmoc-FG wavenumber amide I bands were located with a major maximum peak at 1651 cm^{-1} and at 1700 cm^{-1}. These vibrational peaks are consistent with supramolecular organization of peptide in a non β-sheet conformation. Fmoc-FF wavenumber amide I bands were located with a major maximum peak at 1653 cm^{-1} and a minor peak at 1690 cm^{-1}, Fmoc-2-Nal with a major maximum peak at 1690 cm^{-1}, Fmoc-RGDF with a major maximum peak at 1638 cm^{-1} and minor peaks at 1658 and 1680 cm^{-1}, Fmoc-FRGD with a major maximum peak at 1660 cm^{-1} and minor peaks at 1674 and 1689 cm^{-1} all indicating a high amount of β-conformations (Supporting Information, Figure S5). Fmoc-FP, Fmoc-FS(tBu), Fmoc-GF, and Fmoc-RGD did not exhibit any signal.[51] A summary of the Fmoc-peptides morphological properties is shown in Table 1.

Cell Viability Assay. To verify the ability of the new hydrogels to be used in biological applications, we tested their biocompatibility using an in vitro cell culture experiment. CHO cells were cultivated on top of the gels after their formation in a 96-well culture plate. The cell viability was analyzed following 1, 3, and 7 day incubation periods. CHO cells cultured on uncoated wells were used as control (Figure 5). Cell viability was analyzed using an MTT assay. When MTT was added to the cell culture medium, the mitochondrial dehydrogenase enzyme, which is present only in live cells, changed the color of the yellow MTT to dark-blue crystals, which accumulated inside the living cells and give a clear indication of cell viability.

After one day, the cultured cells on Fmoc-FRGD and Fmoc-RGDF showed a very high viability, whereas the cells on Fmoc-2-Nal showed low viability. However, the number of cells on Fmoc-FRGD and Fmoc-RGDF decreased after three days, whereas Fmoc-2-Nal showed a moderate increase. Seven days after incubation, the number of cultured cells on Fmoc-RGDF remained stable, while a decrease was observed on Fmoc-2-Nal and Fmoc-FRGD. The discrepancy between Fmoc-FRGD

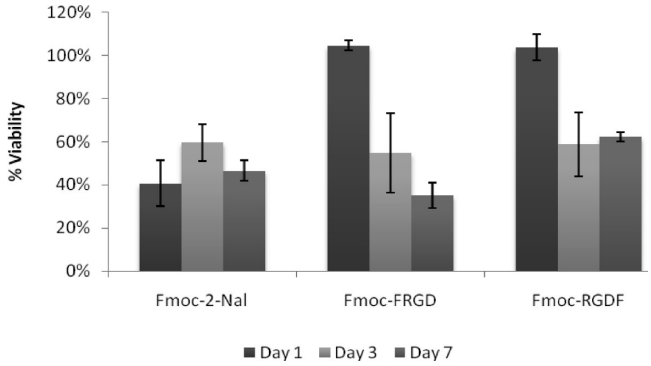

Figure 5. Cell viability test of the new hydrogels for 1, 3, and 7 days.

and Fmoc-RGDF in the viability tests may imply a different arrangement of the Fmoc-peptides and consequently lead to a weaker or stronger cell adhesion capability, respectively. Additionally, the viabilty decrease in the peptides with the RGD sequence was consistent with other observations, which showed a similar decrease in viability during the first seven days.[48] Furthermore, the fact that Fmoc-2-Nal is a synthetic amino acid could contribute to the low viability.

Conclusions

We designed self-assembling peptides by flanking peptides with aromatic moieties. We described and characterized the self-assembly of nine different Fmoc-peptides into various structures with distinctive molecular and physical properties. Each of these nanostructured materials are formed under mild conditions in an aqueous solution using low-molecular weight building blocks. In most cases, their properties enable the utilization in different biomedical applications including drug delivery, tissue engineering, and tissue regeneration, owing to their biocompatibility and assembly into 3D networks. Moreover, we described the fabrication of bioactive RGD peptide hydrogels through their flanking with aromatic moieties. These unique materials offer new opportunities to develope cell-adhesive biomedical hydrogel scaffolds, as well as to establish strategies to modify surfaces with bioactive materials. Electron microscopy analysis revealed a pattern between the micrometer-scaled self-assembled structures of each peptide solution and the bulk viscoelastic properties of their respective final forms. Specifically, fibrous structures formed continuous hydrogels with viscoelastic properties, whereas spheres and discrete tubes remained in a state of viscous solutions. The macro-structure of the hydrogel resembled that of a sponge, which imbibes water along its branched fibers. By comparing a variety of Fmoc-peptides, we have also demonstrated the critical role of aromatic groups in regulating the self-assembly process and consequently influencing the structural and physical properties of the resulting hydrogels. As the number of aromatic groups on the peptide backbone increases, the stiffness of the hydrogels increases and the structural formation occurs with elevated yields. Additional work will be required to appreciate the full potential of this novel class of peptide-based materials in biomedicine and bionanotechnology.

Acknowledgment. E.G. thanks the European Community (BeNatural/NMP4-CT-2006-033256) for financial support. We thank Yaacov Delarea for help with TEM experiments, Dr. Zahava Barkay for help with the SEM experiments, and members of the Gazit and Seliktar laboratories for helpful discussion.

Supporting Information Available. Figure S1 shows the AFM pictures, Figure S2 shows the Congo Red staining, Figure S3 shows the peptides mixture optical change, Figure S4 shows the mixture rheology characterization, and Figure S5 shows FTIR analysis. This material is available free of charge via the Internet at http://pubs.acs.org.

References and Notes

(1) Whitesides, G. M.; Mathias, J. P.; Seto, C. T. *Science* **1991**, *254*, 1312–1319.
(2) Zhang, S. *Nat. Biotechnol.* **2003**, *21*, 1171–1178.
(3) Patolsky, F.; Weizmann, Y.; Willner, I. *Nat. Mater.* **2004**, *3*, 692–695.
(4) Reches, M.; Gazit, E. *Curr. Nanosci.* **2006**, *2*, 105–111.
(5) Mao, C.; Solis, D. J.; Reiss, B. D.; Kottmann, S. T.; Sweeney, R. Y.; Hayhurst, A.; Georgiou, G.; Iverson, B.; Belcher, A. M. *Science* **2004**, *303*, 213–217.
(6) Nam, K. T.; Kim, D. W.; Yoo, P. J.; Chiang, C. Y.; Meethong, N.; Hammond, P. T.; Chiang, Y. M.; Belcher, A. M. *Science* **2006**, *312*, 885–888.
(7) Ghadiri, M. R.; Granja, J. R.; Milligan, R. A.; McRee, D. E.; Khazanovich, N. *Nature* **1993**, *366*, 324–327.
(8) Winfree, E.; Liu, F.; Wenzler, L. A.; Seeman, N. C. *Nature* **1998**, *394*, 539–544.
(9) Zastavker, Y. V.; Asherie, N.; Lomakin, A.; Pande, J.; Donovan, J. M.; Schnur, J. M.; Benedek, G. B. *Proc. Natl. Acad. Sci. U.S.A.* **1999**, *96*, 7883–7887.
(10) Vauthey, S.; Santoso, S.; Gong, H.; Watson, N.; Zhang, S. *Proc. Natl. Acad. Sci. U.S.A.* **2002**, *99*, 5355–5360.
(11) Matsui, H.; MacCuspie, R. *Nano Lett.* **2001**, *1*, 671–675.
(12) Guler, M. O.; Soukasene, S.; Hulvat, J. F.; Stupp, S. I. *Nano Lett.* **2005**, *5*, 249–252.
(13) Yu, L. T.; Banerjee, I. A.; Shima, M.; Rajan, K.; Matsui, H. *Adv. Mater.* **2004**, *16*, 709–712.
(14) Scheibel, T.; Parthasarathy, R.; Sawicki, G.; Lin, X. M.; Jaeger, H.; Lindquist, S. L. *Proc. Natl. Acad. Sci. U.S.A.* **2003**, *100*, 4527–4532.
(15) Aggeli, A.; Bell, M.; Boden, N.; Keen, J. N.; Knowles, P. F.; McLeish, T. C.; Pitkeathly, M.; Radford, S. E. *Nature* **1997**, *386*, 259–262.
(16) Hartgerink, J. D.; Beniash, E.; Stupp, S. I. *Science* **2001**, *294*, 1684–1688.
(17) Madhavaiah, C.; Verma, S. *Chem. Commun.* **2004**, 638–639.
(18) Hartgerink, J. D.; Granja, J. R.; Milligan, R. A.; Ghadiri, M. R. *J. Am. Chem. Soc.* **1996**, *118*, 43–50.
(19) Banerjee, I. A.; Yu, L.; Matsui, H. *Proc. Natl. Acad. Sci. U.S.A.* **2003**, *100*, 14678.
(20) Matsui, H.; Gologan, B. *J. Phys. Chem. B* **2000**, *104*, 3383–3386.
(21) Morikawa, M. A.; Yoshihara, M.; Endo, T.; Kimizuka, N. *Chem. Eur. J.* **2005**, *11*, 1574–1578.
(22) Matsuura, K.; Murasato, K.; Kimizuka, N. *J. Am. Chem. Soc.* **2005**, *127*, 10148–10149.
(23) Reches, M.; Gazit, E. *Nano Lett.* **2004**, *4*, 581–585.
(24) Schneider, J. P.; Pochan, D. J.; Ozbas, B.; Rajagopal, K.; Pakstis, L.; Kretsinger, J. *J. Am. Chem. Soc.* **2002**, *124*, 15030–15037.
(25) Kisiday, J.; Jin, M.; Kurz, B.; Hung, H.; Semino, C.; Zhang, S.; Grodzinsky, A. J. *Proc. Natl. Acad. Sci. U.S.A.* **2002**, *99*, 9996–10001.
(26) Kretsinger, J. K.; Haines, L. A.; Ozbas, B.; Pochan, D. J.; Schneider, J. P. *Biomaterials* **2005**, *26*, 5177–5186.
(27) Aggeli, A.; Bell, M.; Boden, N.; Carrick, L. M.; Strong, A. E. *Angew. Chem., Int. Ed.* **2003**, *42*, 5603–5606.
(28) Yokoi, H.; Kinoshita, T.; Zhang, S. *Proc. Natl. Acad. Sci. U.S.A.* **2005**, *102*, 8414–8419.
(29) Wang, Y.; Ameer, G. A.; Sheppard, B. J.; Langer, R. *Nat. Biotechnol.* **2002**, *20*, 602–606.
(30) Almany, L.; Seliktar, D. *Biomaterials* **2005**, *26*, 2467–2477.
(31) Langer, R.; Vacanti, J. P. *Science* **1993**, *260*, 920–926.
(32) Drury, J. L.; Mooney, D. J. *Biomaterials* **2003**, *24*, 4337–4351.
(33) Silva, G. A.; Czeisler, C.; Niece, K. L.; Beniash, E.; Harrington, D. A.; Kessler, J. A.; Stupp, S. I. *Science* **2004**, *303*, 1352–1355.
(34) Holmes, T. C.; De Lacalle, S.; Su, X.; Liu, G.; Rich, A.; Zhang, S. *Proc. Natl. Acad. Sci. U.S.A.* **2000**, *97*, 6728–6733.
(35) Frey, S.; Richter, R. P.; Gorlich, D. *Science* **2006**, *314*, 815–817.
(36) Ellis-Behnke, R. G.; Liang, Y.-X.; You, S.-W.; Tay, D. K. C.; Zhang, S.; So, K.-F.; Schneider, G. E. *Proc. Natl. Acad. Sci. U.S.A.* **2006**, *103*, 5054–5059.
(37) Vegners, R.; Shestakova, I.; Kalvinsh, I.; Ezzell, R. M.; Janmey, P. A. *J. Pept. Sci.* **1995**, *1* (6), 371–8.

(38) Burch, R. M.; Weitzberg, M.; Blok, N.; Muhlhauser, R.; Martin, D.; Farmer, S. G.; Bator, J. M.; Connor, J. R.; Ko, C.; Kuhn, W.; Mcmillan, B. A.; Raynor, M.; Shearer, B. G.; Tiffany, C.; Wilkins, D. E. *Proc. Natl. Acad. Sci. U.S.A.* **1991**, *88*, 355–359.
(39) Mahler, A.; Reches, M.; Rechter, M.; Cohen, S.; Gazit, E. *Adv. Mater.* **2006**, *18*, 1365–1370.
(40) Smith, A. M.; Williams, R. J.; Tang, C.; Coppo, P.; Collins, R. F.; Turner, M. L.; Saiani, A.; Ulijn, R. V. *Adv. Mater.* **2008**, *20*, 37−41.
(41) Hansen, M. B.; Nielsen, S. E.; Berg, K. *J. Immunol. Methods* **1989**, *119*, 203–210.
(42) Jayawarna, V.; Smith, A.; Gough, J. E.; Ulijn, R. V. *Biochem. Soc. Trans.* **2007**, *35*, 535–537.
(43) Jayawarna, V.; Ali, M.; Jowitt, T. A.; Miller, A. E.; Saiani, A.; Gough, J. E.; Ulijn, R. V. *Adv. Mater.* **2006**, *18*, 611–614.
(44) Rowley, J. A.; Madlambayan, G.; Mooney, D. J. *Biomaterials* **1999**, *20*, 45–53.
(45) Stile, R. A.; Healy, K. E. *Biomacromolecules* **2001**, *2*, 185–194.
(46) Hern, D. L.; Hubbell, J. A. *J. Biomed. Mater. Res.* **1998**, *39*, 266–276.
(47) Mann, B. K.; Gobin, A. S.; Tsai, A. T.; Schmedlen, R. H.; West, J. L. *Biomaterials* **2001**, *22*, 3045–3051.
(48) Zhou, M.; Smith, A. M.; Das, A. K.; Hodson, N. W.; Collins, R. F.; Ulijn, R. V.; Gough, J. E. *Biomaterials* **2009**, *30*, 2523–2530.
(49) Gazit, E. *FASEB J.* **2002**, *16*, 77–83.
(50) Tartaglia, G. G.; Cavalli, A.; Pellarin, R.; Caflisch, A. *Protein Sci.* **2004**, *13*, 1939–1941.
(51) Kong, J.; Yu, S. *Acta Biochim. Biophys. Sin.* **2007**, *39*, 549–559.

BM900584M